

## Scaling of charged particle production and centrality determination in p-Pb collisions at $\sqrt{s_{NN}} = 5.02$ TeV at ALICE

C. Oppedisano<sup>1</sup>, on behalf of the ALICE Collaboration

<sup>1</sup>INFN, Via P. Giuria 1, 10125 Torino, ITALY

**Abstract.** Proton-nucleus collisions are studied in order to disentangle initial state effects, already present in cold nuclear matter, from final state effects, that are associated to the hot and strongly interacting medium created in A-A collisions. However, after the 2013 p-Pb data taking at LHC, the importance of p-A collisions on their own has been acknowledged. Several measurements clearly showed that p-A collisions cannot simply be explained by an incoherent superposition of proton-nucleon collisions, but indicate the presence of coherent and collective effects, with a strong dependence on the collision geometry. These measurements pointed out the need for a detailed characterization of the collision geometry.

Typically, parameters such as the number of binary collisions  $N_{\text{coll}}$  or the number of participating nucleons  $N_{\text{part}}$  are used to characterize the centrality. In nucleus-nucleus interactions the centrality is usually estimated by measuring the charged particle multiplicity. However, in contrast to A-A, in p-A collisions the large fluctuations in a much reduced multiplicity environment generate a dynamical bias in centrality classes based on particle multiplicity measurement.

The centrality determination is critically addressed and a different approach to extract the average  $N_{\text{coll}}$  values, needed to compare p-A to pp data, is presented. The centrality dependence of primary charged-particle production and of transverse momentum distributions in p-A collisions at  $\sqrt{s_{NN}} = 5.02$  TeV measured by ALICE are presented.

### 1 Introduction

Proton-lead collisions are an essential component of the heavy ion programme at LHC. These collisions are needed as a baseline in the understanding of cold nuclear matter effects and therefore in the interpretation of the nucleus-nucleus data. However, the importance of p-Pb collisions at LHC on their own has soon been recognized. In fact several measurements [1]-[4] clearly indicate that p-Pb collisions can not be explained as a simple incoherent superposition of proton-nucleon collisions, but rather indicate the onset of collective effects with a strong collision geometry dependence. The study of key observables as a function of centrality poses a crucial focus on the centrality determination. One of the main observables used to study p-A collisions is the nuclear modification factor:

$$R_{pA} = \frac{dN^{p\text{-Pb}}/dp_T}{\langle N_{\text{coll}} \rangle \cdot dN^{pp}/dp_T} \quad (1)$$

The  $R_{pA}$  compares the yield in p-Pb to the yield in p-p scaled by the average number of binaries proton-nucleon collisions in centrality selected samples. For the minimum bias sample, the average  $N_{\text{coll}}$  can be calculated from the ratio of p-N and p-A inelastic cross-sections:  $\langle N_{\text{coll}} \rangle^{MB} = A \cdot \sigma_{pN} / \sigma_{pA} = 6.9$  [5]. For the analysis as a function of centrality, the details of centrality determination procedure becomes crucial.

## 2 Centrality determination: common approach

To determine the relation between a measured observable and the collision geometry, typically defined through the number of participating nucleons  $N_{\text{part}}$  or the number of binary collisions  $N_{\text{coll}}$ , usually a Glauber model is used in combination with a model that accounts for particle production. This kind of approach has already been used by ALICE for the centrality determination in Pb-Pb [6].

In ALICE, the centrality can be estimated by measuring either the charged particle multiplicity or the energy detected at zero degrees. At midrapidity the multiplicity can be measured by the innermost silicon pixel layers of the Inner Tracking System (ITS), specifically the number of clusters measured in the second layer ( $|\eta_{LAB}| < 1.4$ ) is used as an estimator, named CL1. At more forward rapidities, 2 scintillator hodoscopes placed on both sides relative to the interaction point (IP) have been employed: VOA placed on the Pb-remnant side ( $2.0 < \eta_{LAB} < 5.1$ ) and VOC on the proton remnant side ( $-3.7 < \eta_{LAB} < -1.7$ ). At very forward rapidities the Zero Degree Calorimeters (ZDC), placed at  $\pm 112.6$  m from the IP, detect the energy carried by nucleons knocked out or emitted in de-excitation processes by the interacting nucleus, usually called “slow” nucleons [7] (and references therein). Each ZDC set is composed by a neutron (ZN) and a proton (ZP) calorimeter.

Charged particle production is typically modeled using a Negative Binomial Distribution (NBD), assuming  $N_{\text{part}}$  as the number of particle sources (ancestors). For the zero degree energy, a model to account for the slow nucleon (SNM) emission is coupled with the Glauber Monte Carlo. The SNM we used is a heuristic model based on experimental results at lower energies, where it has been reported that the features of the emitted nucleons weakly depend on the incident proton beam energy in a rather wide range from 1 GeV to 1 TeV [7].

From the Glauber model, the probability  $\pi(\nu)$  for having  $\nu$  binary collisions (or participants) is obtained. Then, from the coupled model for particle emission, one can calculate the probability to observe a multiplicity  $M$  for a given  $\nu$ ,  $\mathcal{P}(M|\nu)$ . The multiplicity or zero degree energy value obtained in this way is then fitted to experimental data. Finally, centrality classes are defined slicing the measured distributions, and the information from the Glauber MC in the corresponding generated distributions is used to calculate the mean number of participants  $\langle N_{\text{part}} \rangle$  and the mean number of binary collisions  $\langle N_{\text{coll}} \rangle$ .

In figure 1 VOA multiplicity and ZNA energy are shown with, superimposed, the results from the Glauber fit. For VOA the fit is performed excluding the 90-100% region to avoid the region with lower trigger efficiencies. The values of the NBD parameters are similar to those obtained fitting the corresponding multiplicity in pp collision at  $\sqrt{s} = 7$  TeV. The SNM implementation allows to reproduce the essential features of the ZN spectrum, such as the low neutron multiplicity peaks and the observed saturation. The average values of  $N_{\text{coll}}$  estimated through the Glauber approach using different estimators are shown in figure 2. Values from the different estimators agree within the systematic uncertainty (estimated by varying the Glauber parameters and with a MC closure test using HIJING).

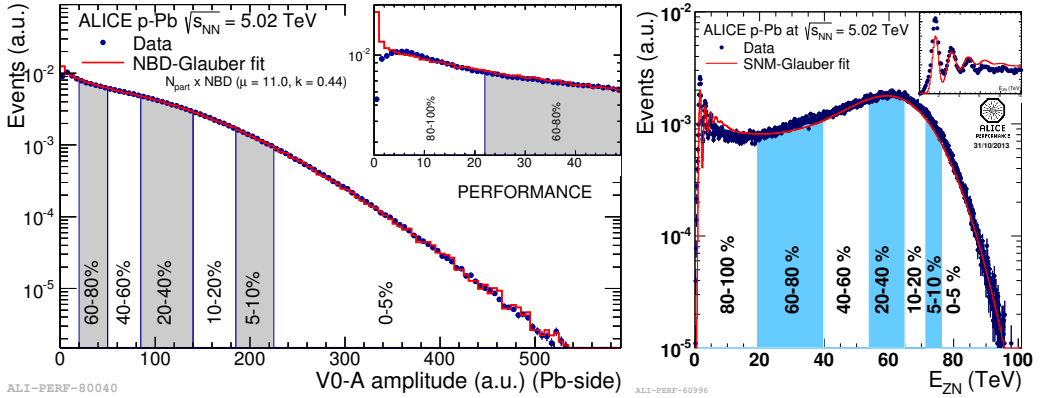


**Figure 1.** Left: amplitude of V0A signal fitted with NBD+Glauber function. Right: ZNA spectrum with SNM+Glauber fit superimposed.

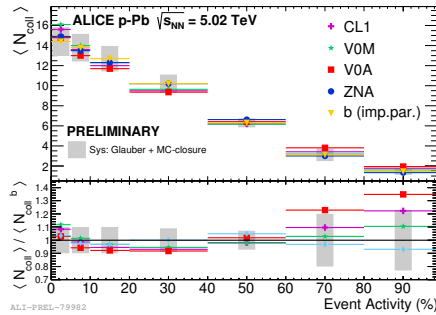


**Figure 2.**  $\langle N_{coll} \rangle$  values obtained from Glauber fit approach applied to different estimators and by selecting events on the pure Glauber MC in impact parameter  $b$ .

### 3 Biases affecting the centrality determination

Three possible sources that can induce biases on the centrality determination based on charged particle multiplicity measurements have been identified. They are addressed in this Section.

#### 3.1 Multiplicity bias

For centrality estimators based on charged particle measurements, one has to consider that, in contrast to Pb-Pb collisions, for p-Pb interactions the large multiplicity fluctuations for a fixed  $N_{part}$  value are sizable compared to the width of the  $N_{part}$  distribution (see figure 3). The presence of such large fluctuations generates a dynamical bias in centrality classes based on particle multiplicity and may select a biased sample of nucleon-nucleon collisions. Such a bias occurs for any system with large relative statistical fluctuations, and it can be quantified using the Glauber fit itself. In the left panel of figure 4 the ratio between the average multiplicity per ancestor from Glauber and the average NBD multiplicity is shown as a function of centrality. While in Pb-Pb it deviates from unity only for very

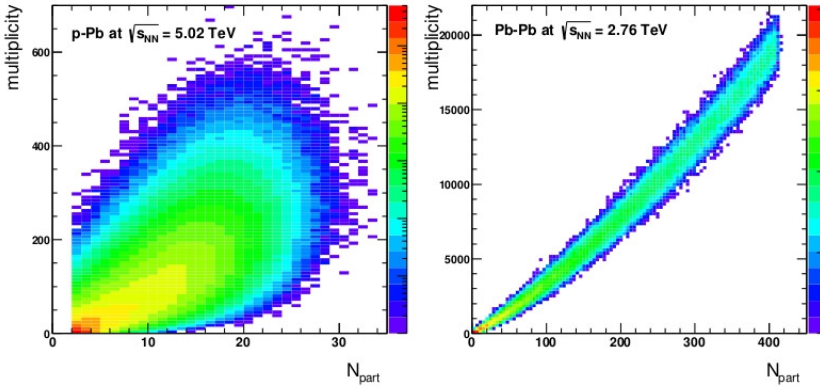


**Figure 3.** Correlation between the charged particle multiplicity and number of participating nucleons in p-Pb (left) and in Pb-Pb (right) collisions from Glauber Monte Carlo.

peripheral events, in p-Pb collisions we observe large deviations over the whole centrality range. The most central (peripheral) collisions have on average much higher (lower) multiplicity per ancestor.

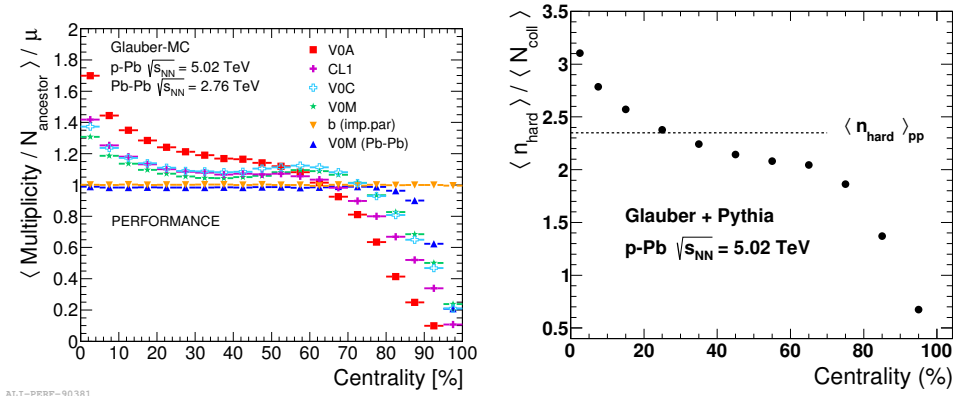


**Figure 4.** Left: multiplicity fluctuation bias calculated from NBD-Glauber MC as the ratio between mean multiplicity per ancestor and mean NBD multiplicity. Right: number of hard scatterings per  $N_{\text{coll}}$  as a function of centrality as calculated with a toy MC that couples p-Pb Glauber MC to PYTHIA6 pp events.

In all recent Monte Carlo generators a large part of the multiplicity fluctuations is due to the fluctuations of the number of particle sources, i.e. Multiple semi-hard Parton Interactions (MPI). As an example, the HIJING generator accounts for fluctuations of the number of MPI per NN interaction via an NN overlap function  $T_{\text{NN}}(b_{\text{NN}})$ , where  $b_{\text{NN}}$  is the NN impact parameter, i.e. the impact parameter between the proton and each wounded nucleon of the nucleus. The average number of hard scatterings depends on  $b_{\text{NN}}$  through  $\langle n_{\text{hard}} \rangle = \sigma_{\text{hard}} T_{\text{NN}}(b_{\text{NN}})$ . However, in HIJING the total number of hard scatterings deviates from a binary scaling due to energy conservation at high  $N_{\text{coll}}$ . Therefore, to study a baseline based on an incoherent and unconstrained superposition of nucleon-nucleon collisions,

PYTHIA6 (Perugia 2011 tune) [9] was coupled to the p-Pb Glauber MC calculation. For each  $N_{\text{coll}}$  value from the Glauber distribution, a corresponding number of independent PYTHIA pp events is superimposed. We refer to this toy MC as G-PYTHIA hereafter. In the right panel of figure 4 the average number of hard scatterings per collision obtained from G-PYTHIA is shown as a function of centrality. Deviations from the binary scaling are observed over the whole centrality range, with a behavior resembling the bias in multiplicity obtained from the Glauber MC (shown in the left panel of figure 4). Therefore the bias on the multiplicity corresponds to a bias on the number of particle sources (ancestors in NBD-Glauber approach, hard scattering in more sophisticated models).

### 3.2 Jet-veto effect

A kinematic bias arises in events containing high  $p_T$  particles. These particles contribute to the overall event multiplicity and can thus introduce trivial correlations between centrality estimators based on multiplicity measurements and the presence of high  $p_T$  particles in the event. In particular, for very peripheral collisions, the multiplicity range that governs the centrality for the bulk of soft collisions can represent an effective veto on hard processes, leading to a  $R_{pA} < 1$ . This effect is expected to be most important for CL1 estimator that has a full overlap with the tracking region.

### 3.3 Geometric bias

Finally, a purely geometrical bias, independent on the considered centrality estimator, has to be considered for peripheral collisions. This is due to the fact that the mean impact parameter between two nucleons ( $b_{NN}$ ), calculated from a Monte-Carlo Glauber simulation, is almost constant for central collisions, but rises significantly for peripheral interactions. This reduces the average number of MPIs for most peripheral events, enhancing the effect of the bias leading to a nuclear modification factor less than one for peripheral collisions.

In summary, three different possible sources of bias have been identified. They are expected to lead at high  $p_T$  to deviations from unity of the nuclear modification factors both in peripheral and in central collisions. As will be discussed in the following sections, the effects decrease with increasing rapidity separation between the  $p_T$  spectrum measurements and the centrality estimator.

## 4 Biased nuclear modification factors

All these sources of bias imply that the average  $N_{\text{coll}}$  from the Glauber approach can not be used to scale pp data and compute nuclear modification factors. For this reason we define a “biased” nuclear modification factor:

$$Q_{pPb} = \frac{dN_{pPb}/dp_T}{N_{\text{coll}}^{\text{Glauber}} dN_{pp}/dp_T}$$

that will differ from unity at high  $p_T$  due to the identified biases even if the binary scale holds. In figure 5 the  $Q_{pPb}$  for charged primary particles is shown in 7 centrality bins for CL1 and for V0A estimators. As expected, the ratio differs from unity at high  $p_T$ . There is also a clear indication of the jet-veto effect in the most peripheral CL1 class where  $Q_{pPb}$  has a negative slope with increasing  $p_T$  due to the fact that the jet contribution to the overall multiplicity increases with  $p_T$ . The spread between different centrality classes is reduced increasing the rapidity gap between the region where the tracking is performed (midrapidity) and the centrality estimator. This can be inferred by comparing the results obtained using CL1 (full overlap) and V0A (larger  $\eta$  gap) estimators.

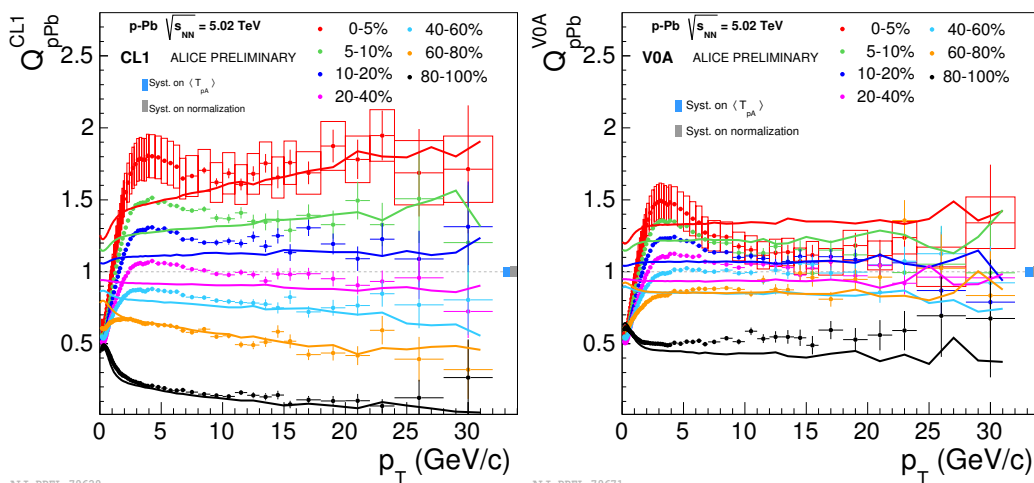


**Figure 5.**  $Q_{pPb}$  spectra of charged primary particles for CL1 estimator (left) and V0A estimator (right). The closed points are the data, the lines are the results from G-PYTHIA.

Results from G-PYTHIA calculations are also shown. A good agreement with data for all centrality classes is observed, in particular for CL1 estimator. This suggests that the proper scaling for high  $p_T$  particle production is an incoherent superposition of pp collisions. The agreement is worse for V0A estimator since the model is not adequate for forward particle production, in particular in the Pb fragmentation region where V0A is located. G-PYTHIA reproduces also the jet-veto bias in the most peripheral CL1 bin.

## 5 A new approach for centrality determination

To provide an unbiased centrality selection, an alternative, entirely data driven method has been developed. This is based on two main assumptions. The first one is to assume that selecting events with the neutron ZDC (ZN) does not induce any bias. To obtain more insight into the particle production mechanism, we studied the correlation of various observables that are expected to scale linearly with  $N_{part}$  or  $N_{coll}$ , in bins of ZN centrality. To compare the different observables on the same scale, we considered the signals normalized to their minimum bias (MB) values:  $S_i/\langle S_{MB} \rangle$ . In the left panel of figure 6 the correlation between a few selected normalized signals and the normalized charged-particle density averaged over  $-1 < \eta < 0$  is shown. The charged particle pseudorapidity density is obtained from the measured distribution of tracklets, formed using the position of the primary vertex and two hits, one on each SPD layer [12]. The statistical uncertainty is negligible, while the systematic uncertainties largely cancel in the ratio to the MB signals. The correlation exhibits a clear dependence on pseudorapidity. The slope of the normalized signals diminishes towards the proton direction (V0C side).

In order to further quantify the relative trends of the observables and to relate them with geometrical quantities, such as  $N_{part}$ , we use the Wounded Nucleon Model [10] assumption that  $dN_{ch}/d\eta$  at

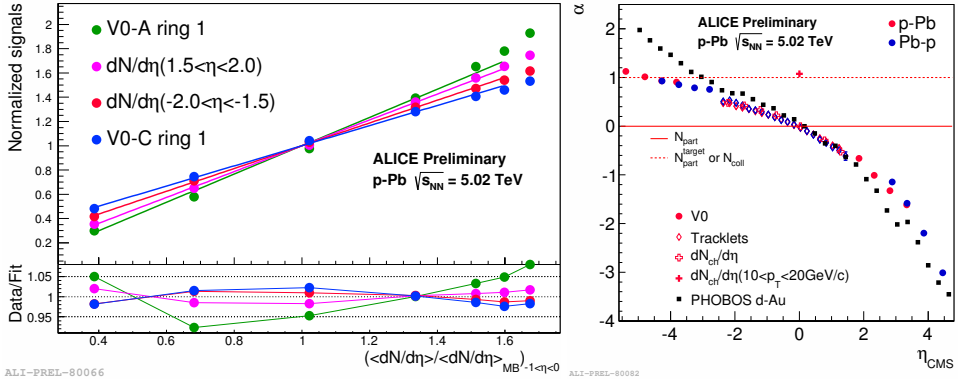


**Figure 6.** Left: normalized signals from various observables (innermost V0A ring, V0C and two rapidity intervals of  $dN_{ch}/d\eta$ ) versus the normalized charged-particle density in  $-1 < \eta < 0$ . Right: Result for the  $\alpha$  parameter from the linear fit 2. Negative pseudorapidity values correspond to the Pb-going side.

midrapidity is proportional to  $N_{part}$ . We fit the different observables with a linear function:

$$\frac{\langle S \rangle_i}{\langle S \rangle_{MB}} = \frac{\langle N_{part} \rangle_{MB}}{\langle N_{part} \rangle_{MB} - \alpha} \cdot \left( \frac{\langle dN/d\eta \rangle_i}{\langle dN/d\eta \rangle_{MB}} \right)_{-1 < \eta < 0} - \frac{\alpha}{\langle N_{part} \rangle_{MB} - \alpha} \quad (2)$$

The value of the free parameter  $\alpha$  for each observable is extracted from a fit to the data and shown in the right panel of figure 6. A perfect  $N_{part}$  scaling holds for  $\alpha = 0$ . A clear and smooth change of the scaling behaviour for charged particle production as a function of the covered pseudorapidity can be observed. In the Pb-going direction the value of the  $\alpha$  parameter reaches the value obtained for charged-particle production at high- $p_T$ , which is a signature of  $N_{part} + 1 = N_{coll}$  scaling. Our data are overlaid with the fit parameters derived from PHOBOS charged-particle multiplicity measurements [11], scaled by the ratio of the beam rapidities in p-Pb at  $\sqrt{s_{NN}} = 5.02$  TeV and in d-Au collisions at  $\sqrt{s_{NN}} = 200$  GeV.

The second assumption of the model is based on these findings on the scaling of charged particle production as a function of rapidity. We make three hypothesis on observables that are expected to scale as a linear function of  $N_{coll}$  or  $N_{part}$ , obtaining thus 3 sets of  $\langle N_{coll} \rangle$  values:

1.  $N_{coll}^{mult}$  assuming that  $dN_{ch}/d\eta$  at mid-rapidity is proportional to  $N_{part}$ :

$$\langle N_{coll} \rangle_i^{mult} = \langle N_{part} \rangle_{MB} \cdot \left( \frac{\langle dN/d\eta \rangle_i}{\langle dN/d\eta \rangle_{MB}} \right)_{-1 < \eta < 0} - 1 \quad (3)$$

2.  $N_{coll}^{high-pr}$  assuming that the yield of charged high- $p_T$  particles at mid-rapidity is proportional to  $N_{coll}$ :

$$\langle N_{coll} \rangle_i^{high-pr} = \langle N_{coll} \rangle_{MB} \cdot \frac{\langle S \rangle_i}{\langle S \rangle_{MB}} \quad (4)$$

3.  $N_{coll}^{Pb-side}$  assuming that the Pb-side charged-particle multiplicity is proportional to the number of wounded target nucleons ( $N_{part}^{target} = N_{part} - 1 = N_{coll}$ ):

$$\langle N_{coll} \rangle_i^{Pb-side} = \langle N_{coll} \rangle_{MB} \cdot \frac{\langle S \rangle_i}{\langle S \rangle_{MB}} \quad (5)$$

The first two conditions are satisfied for minimum bias collisions [12], [13]. The obtained  $N_{\text{coll}}$  values are in good agreement, with differences within 10%, showing the consistency of the three hypothesis even if not providing a proof for their validity.

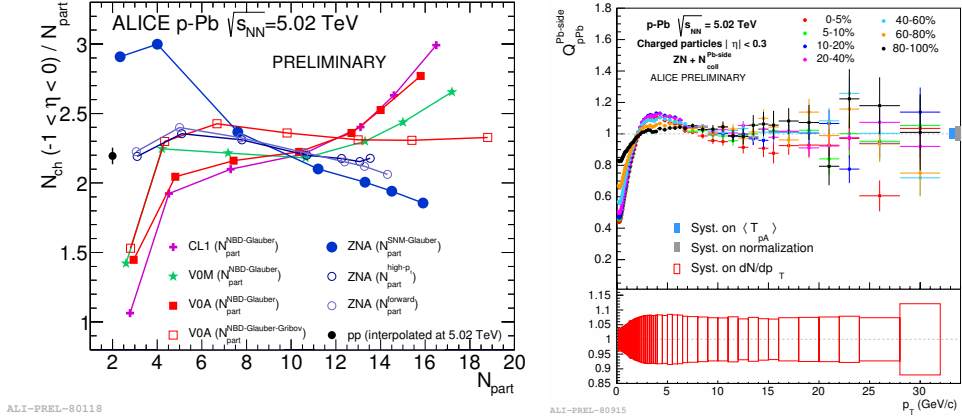


**Figure 7.** Left: Pseudorapidity density of charged particles produced at midrapidity per participant as a function of  $N_{\text{part}}$ . Right:  $Q_{\text{pPb}}$  for charged primaries in ZNA centrality classes using  $N_{\text{coll}}^{\text{Pb-side}}$  set.

Figure 7, on the left panel, shows  $dN/d\eta$  integrated at midrapidity divided by the number of participants as a function of  $\langle N_{\text{part}} \rangle$  for various centrality estimators. For the VOA centrality estimator, in addition to the  $\langle N_{\text{part}} \rangle$  from the standard Glauber calculation, also those obtained with the implementation of Glauber-Gribov model [14] are shown. For the standard Glauber calculations, the charged particle density at midrapidity increases more than linearly, as a consequence of the strong multiplicity bias. The effect is more pronounced using CL1 estimator, since there is a complete overlap with the tracking region. This trend is absent in the case of the Glauber-Gribov model, which shows a relatively constant behaviour, with the exception of the most peripheral point, that does not reach the pp value. The results obtained with the proposed alternative method, using  $N_{\text{part}}^{\text{Pb-side}}$  and  $N_{\text{part}}^{\text{high-}p_T}$  sets, do not depend on centrality and they reach the pp value. The  $Q_{\text{pPb}}$  spectra calculated using ZNA centrality selection and the two assumptions on midrapidity and forward rapidity particle production (and not the one on high  $p_T$  particle production) give very similar results (see figure 7, left panel where  $Q_{\text{pPb}}$  spectra for charged particles are shown for the  $N_{\text{coll}}^{\text{Pb-side}}$  assumption). The effects observed in Figure 5 due to the biases are no more present: the spectra for different centrality bins are in good agreement and they are consistent with unity at high  $p_T$ .

The average  $Q_{\text{pPb}}$  at high  $p_T$  as a function of centrality is shown in figure 8. For estimators based on charged particle multiplicity (left panel), the centrality dependence shows the multiplicity bias that is also reproduced by the G-PYTHIA calculations (superimposed lines). With the new approach, the centrality dependence is washed out and the results with two different assumptions on particle production are both consistent with unity. This also demonstrates that each of the hypothesis made on particle production implies the other two.

## 6 Conclusions

Centrality estimators based on particle multiplicity measurements induce a bias on the hardness of p-N collision. The bias effects can be reduced by increasing the rapidity gap between the tracking region



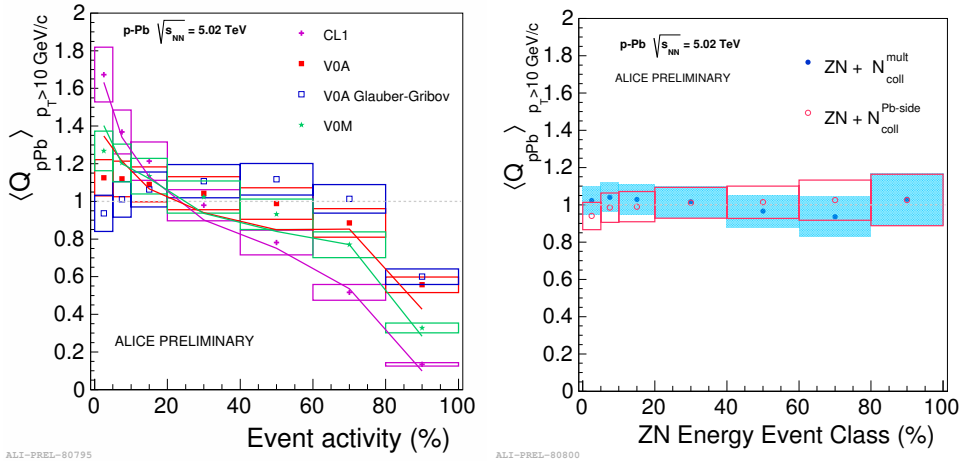


**Figure 8.** Average  $Q_{pPb}$  for  $p_T > 10 \text{ GeV}/c$  as a function of centrality, using the biased estimators (right) and with the new method (right). Lines are from G-PYTHIA calculations.

and the multiplicity estimator. The smallest bias is expected to hold for the ZNA estimator since the slow nucleon emission is independent of hard processes. A data driven approach for centrality determination in p-A collisions at LHC energies has been presented. It relies on an event selection based on ZN energy and three different and independent assumptions for particle productions. The results obtained within this approach do not show the biases observed for centrality estimators based on particle measurements at mid- or forward rapidities.

## References

- [1] ALICE Collaboration, Phys. Lett. **B719**, 29 (2013)
- [2] ALICE Collaboration, Phys. Lett. **B726**, 164 (2013)
- [3] ALICE Collaboration, Phys. Lett. **B727**, 371 (2013)
- [4] ALICE Collaboration, Phys. Lett. **B728**, 25 (2014)
- [5] ALICE Collaboration, Phys. Rev. Lett. **110** 2013 082302
- [6] ALICE Collaboration, Phys. Rev. C **88**, 044909
- [7] F. Sikler, arXiv:hep-ph/0304065
- [8] X.-N. Wang and M. Gyulassy, Phys. Rev. D **44**, 3501 (1991)
- [9] P. Skands, Phys. Rev. D **82**, 074018 (2010)
- [10] A. Bialas and A. Bzdak, Phys.Rev. C **77**, 034908 (2008)
- [11] PHOBOS Collaboration, Phys.Rev. C **72**, 031901 (2005)
- [12] ALICE Collaboration, Phys. Rev. Lett. **110**, 032301 (2013)
- [13] ALICE Collaboration, Phys. Rev. Lett. **110**, 082303 (2013)
- [14] V. Gribov, Sov. Phys. JETP **29**, 483 (1969)